# Flow Induced Vibration Measurement Techniques for Nuclear Fuel Rod Buddle and Wall

Wenyao Ma, Runheng Zuo, Jiyan Li and SAQIB ALI

***Abstract*—Fuel rods are critical for the normal operation and safety of nuclear reactors. High-flow-induced vibrations (FIV) impose significant constraints on these rods, potentially leading to material fatigue, wear, and even failure. We have investigated advanced technologies for measuring the vibrations of nuclear fuel rods. An overview and evaluation of the working principles and applicability of Fiber Bragg Grating (FBG) sensors, Laser Doppler Vibrometers (LDV), Micro-electromechanical Systems (MEMS) accelerometers, Eddy Current sensors, and grid method (GRID) were conducted. Both LDV and MEMS accelerometers demonstrated their value in our study; the former provides precise non-contact measurements, while the latter offers unrestricted measurement locations and performs well under dynamic conditions. A 3×3 rod bundle model was established, and the vibrations of the glass wall and each rod needed to be measured. In our measurement system, LDV was employed to measure the vibration intensity of the glass wall and external rods, offering high spatial distribution and high temporal resolution non-invasive data capture capabilities. MEMS-based accelerometers were affixed to the inside surface of the rods to get extensive vibration coverage using near-field data. The experimental arrangement placed significant emphasis on achieving dependable data synchronization, highlighting the crucial role of precision and compensating for system errors. The study findings suggest that employing sophisticated measuring techniques is crucial for investigating the vibrations caused by fluid flow in nuclear fuel rods, a matter of utmost importance for ensuring the safety of reactors. Utilizing advanced sensors for ongoing monitoring, enhancing vibration measuring techniques can result in improved diagnostics, safer nuclear energy solutions, and predictive maintenance. This can facilitate the enhancement of design enhancements for future study.**

***Index Terms*—Flow induced vibration, vibration measurement, Laser Doppler Vibrometer, MEMS accelerometer**

## I. Introduction

Flow Induced vibration (FIV) in nuclear power plants poses significant challenges to the safe operation of reactors, especially in advanced reactor designs such as the Supercritical Water Cooled Reactor (SCWR) [1]. Vibration of the fuel rod bundle can lead to Pellet Cladding Interaction (PCI) [2], which not only reduces the service life of the fuel rods but also poses the risk of radioactive material leakage. In the SCWR design, a cooler located at the top of the pressure tube is responsible for removing fission and gamma energy, while the pressure tube is connected to cooling pumps and safety auxiliary systems to form a supercritical water loop that simulates the supercritical water environment around the fuel assembly, as Fig. 1 shows. The design of this system must fully consider the vibration behavior of fuel rods in the supercritical water environment to ensure their integrity and the safety of the reactor. Therefore, a thorough investigation and understanding of FIV phenomena are crucial for the design, operation, and maintenance of nuclear power plants.

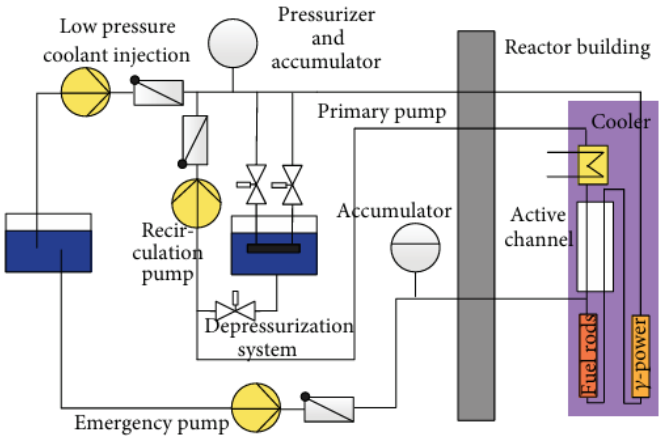


Fig. 1. Concept of the active channel for SCWR fuel qualification [1].

Generally, addressing the FIV issues in nuclear power plants requires precise measurement techniques [3]. This includes detailed analysis of the vibration characteristics of fuel rod bundles and containment structures, as well as the development of effective vibration control strategies. Low frequency vibrations, high frequency vibrations, and resonance can all occur, with the ratio between the upper and lower limits of the vibration frequency range exceeding 30-fold [4]. Consequently, the measurement system needs to cover a sufficiently wide range of vibrations. Additionally, the small diameter of the fuel rods and the narrow spacing between them pose challenges for the size and placement of contact-based vibration sensors. The vibrations of the outer fuel rod bundles have been extensively studied. Optical measurement methods have proven to be sufficiently accurate for these measurements [4]–[6]. However, measuring the vibrations of the inner rod bundles remains a challenge because optical measurement methods cannot directly focus on the inner bundles due to obstruction by the outer bundles. Contact-based measurement methods are generally considered to be a more feasible solution [7].

Given the critical need of exact vibration measurements for the safe running of nuclear power plants, our study presents a complex measuring system using both contact and non-contact techniques. Apart from the mentioned methods, we use sophisticated signal processing systems to improve the dependability and accuracy of our data even further. This covers machine learning methods for predictive maintenance and anomaly identification as well as Kalman filtering and

wavelength transformations for efficient noise reduction and signal enhancement. We hope to build a complete monitoring system able to precisely detect and quantify vibrations as well as forecast any problems by including these modern technologies. This method guarantees that our measuring system can fit the dynamic and complicated surroundings of a supercritical water-cooled reactor, thereby prolonging the fuel rod lifetime and lowering the radioactive material leakage risk.

Before carrying out our project, we will introduce a series of vibration measurement methods. Non-contact techniques, such as Laser Doppler Vibrometer (LDV) [8] and the grid method (GRID) [9], provide high-precision vibration velocity data without interfering with the measured object. In contrast, contact methods, including resistive or capacitive Micro-Electro-Mechanical Systems (MEMS) [10] and Fiber Bragg Grating (FBG) [11], measure vibration acceleration and strain by directly attaching to the structure, allowing detection of a wider range of vibration locations. Traditional non-contact vibration measurement techniques, such as Eddy Current Sensors [12], are also considered. We particularly focus on the principles, advantages, and disadvantages of these measurement techniques, which aids in the better design of our measurement system.

In our measurement system, both the LDV and MEMS accelerometer are selected. The MEMS accelerometer is used for contact measurements of the vibrations of the glass wall and various rods (including both internal and external rods). The LDV is utilized for non-contact measurements of the vibrations of the glass wall and external rods. The MEMS is chosen because of the small size, low cost and high accuracy [13], [14], and LDV is used for its ultra-high accuracy [15]. However, our measurement system using MEMS is sufficient to measure the vibrations of all rods and glass wall, and the high price of LDV makes it optional.

A MEMS accelerometer array is used to measure the vibrations of all devices. The glass wall and each rod are equipped with multiple MEMS accelerometers. There are multiple layers of sensors along the direction of the rods. In detail, on each layer, three MEMS are uniformly distributed on each rod, and four MEMS are uniformly distributed on the glass wall. With this structure, we can accurately measure vibrations at multiple points. And With the help of multi-sensor data fusion technology [16], [17], we can achieve error compensation. The multi-layer structure facilitates the exploration of vibration distribution along the rods. For LDV, it is mounted on the optical table to measure the vibrations of the external rods, the direction can be changed to measure the vibrations in two dimensions. Of course, it can also measure the vibration of the glass wall, just stick a reflective tape on the glass wall.

The data processing involves collecting acceleration data from the MEMS and velocity data from the LDV, filtering the raw data to remove noise, and applying Fourier transforms to convert these signals into the frequency domain. This transformation enables the analysis of dominant frequencies and vibration modes, and the use of advanced multi-sensor data fusion algorithms refines the data, ensuring accurate and comprehensive vibration measurements.

The IIS2DH MEMS accelerometer model (STMicroelectronics N.V., Switzerland) with its extremely small size and adjustable range, and the OFV5000 ultra-high precision LDV model (Polytec GmbH, Germany) were selected for vibration measurement. The JX-3B exciter model (Beijing Instrument Industry Co., Ltd., China) was used to excite the vibration and calibrate the sensors. Without using the LDV and exciter, our measurement system, which includes 62 MEMS accelerometers and other minor components, costs about CNY 1,580. In contrast, when the LDV and exciter are used, the total cost is about CNY 194,630.

## II. Review of Vibration Measurement Techniques

### A. Fiber Bragg Grating (FBG)

Fiber Bragg Grating (FBG) is a sophisticated optical sensing technology that leverages the reflection characteristics of a periodically varied refractive index within an optical fiber to measure strain. FBG sensors determine the strain or temperature changes experienced by the fiber by detecting minute changes in the reflected wavelength, which correspond directly to the physical state of the fiber grating [18].

*1) Principles of FBG:* Fig. 2 shows the core principle behind FBG, which is based on the reflection of light and the Bragg condition. When light propagates through the fiber, only the wavelength that satisfies the Bragg condition is reflected, while other wavelengths are transmitted. The Bragg condition is given by

$$\lambda_B = 2n \cdot \Lambda \tag{1}$$

where $\lambda_B$ is the Bragg wavelength, $n$ is the effective refractive index of the fiber core, and $\Lambda$ is the grating period.

The reflected wavelength changes with strain and temperature variations in the fiber, allowing FBG sensors to measure these physical quantities. The changes in the Bragg wavelength due to strain and temperature are described as

$$\frac{\Delta\lambda}{\lambda_o} = (1 - p_e) \cdot \epsilon + (\alpha_\Lambda + \alpha_n) \cdot \Delta T \tag{2}$$

Where $\frac{\Delta\lambda}{\lambda_o}$ reflects the wavelength shift over initial reflection wavelength due to $\epsilon$ strain, $\Delta T$ temperature change, characterized by the strain optical sensitivity $p_e$, the thermal expansion coefficient $\alpha_\Lambda$, and the temperature optical sensitivity $\alpha_n$.

Fig. 2 shows Fiber Bragg Grating (FBG) sensors, which leverage the periodic refractive index variations within an optical fiber to detect changes in the reflection characteristics of light, can be utilized to accurately capture the vibrations of fuel rods.

In the context of nuclear power plants, FBG sensors can be used to measure the dynamic strain of a fuel rod bundle, thereby inferring its vibration. The sensors can be attached to the surface of the fuel rods, and by detecting changes in the reflected light's wavelength, the vibration of the rod bundle can be monitored.

*2) Advantages of FBG:* Generally speaking, FBG sensors offer several advantages like high sensitivity, immunity to electromagnetic interference, small size, lightweight, and the capability for remote monitoring [4].

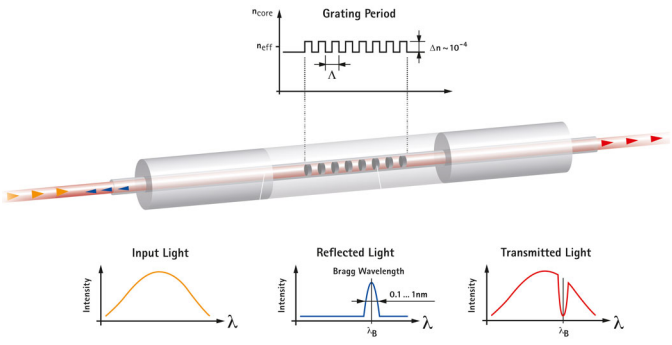


Fig. 2. Schematic diagram of FBG principle [18].

*3) Disadvantages of FBG:* However, these benefits come at the cost of requiring complex demodulation equipment and algorithms to accurately extract measurement data, as well as precise compensation techniques for their cross-sensitivity to temperature and strain [5].

### B. Laser Doppler Vibrometer (LDV)

Laser Doppler Vibrometry (LDV) is a non-contact measurement technique used to determine the velocity and displacement of vibrating surfaces. Unlike traditional contact-based methods, LDV utilizes the Doppler effect of laser light reflected from a moving surface to measure vibrations with high precision and accuracy. This technology is especially advantageous in situations where attaching sensors is impractical or impossible, such as with delicate, high-temperature, or rotating objects [8], [19], [20].

*1) Principles of LDV:* Fig. 3 shows the core principle behind LDV, which is the Doppler effect, named after the Austrian physicist Christian Doppler, who first described the phenomenon in 1842. When a laser beam is directed at a vibrating surface, the frequency of the reflected light is shifted proportionally to the velocity of the surface along the line of sight of the laser beam. This frequency shift, $f_D$, is given by

$$f_D = \frac{2v}{\lambda} \tag{3}$$

where $v$ is the velocity of the surface, and $\lambda$ is the wavelength of the laser light.

The frequency shift can be detected by comparing the frequency of the reflected light with the frequency of a reference beam using heterodyne detection. The relationship between the phase $\phi(t)$ of the electrical field $E(t)$ and the displacement $s(t)$ of the vibrating surface is expressed as

$$\phi(t) = \phi_0 - \frac{4\pi}{\lambda} s(t) \tag{4}$$

Taking the time derivative of the phase gives the instantaneous velocity $v(t)$, which is $\dot{\phi}(t) = -\frac{4\pi}{\lambda} v(t)$. Thus, the Doppler frequency shift $f_D$ is

$$f_D = \frac{\dot{\phi}(t)}{2\pi} = -\frac{2v(t)}{\lambda} \tag{5}$$

LDV systems typically use interferometric methods to measure the phase difference between the reference and measurement beams. The electric field of the measurement beam

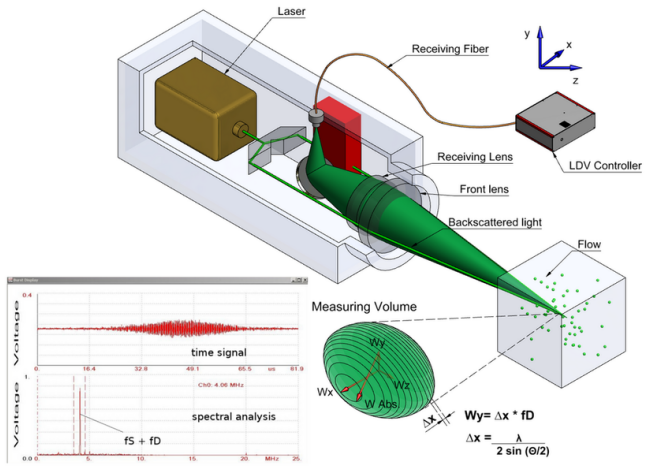


Fig. 3. Schematic diagram of LDV principle [21].

$E_m(t)$ and reference beam $E_r(t)$ are combined, and the resulting interference pattern is detected by a photodetector.

In heterodyne interferometry, the frequency of the measurement beam is shifted by a carrier frequency $\omega_c$, producing a beat frequency when mixed with the reference beam. The detector signal $u(t)$ is then

$$u(t) = A\cos(\omega_c t + \phi(t)) \tag{6}$$

where $A$ is the amplitude of the combined signal. The phase $\phi(t)$ is directly related to the surface displacement [19].

For the detection of vibration dynamics in the frequency range from a few hertz up to several megahertz, Laser Doppler Vibrometry (LDV) provides an accurate and reliable technology. This technology uses laser light to accurately measure speed and position without needing to touch the component. It can record motions as small as picometers and speeds of a few micrometers per second. Use of LDV is especially useful when conventional contact sensors are unsuitable, e.g. when the temperature is very high, the structure is distortable or the components are moving. The LDV is a much more popular tool for this purpose because of its high precision and versatility, and has been applied to the measurement of many things, including to the measurement of the vibration of nuclear fuel rods, aeronautical engineering, microelectronics and structural health monitoring etc. This will also serve in the both performance and design part.

*2) Advantages of LDV:* LDV offers several significant advantages. One of the primary benefits is that it allows for non-contact measurement, which means that the vibrometer does not need to touch the surface being measured. This is particularly advantageous for measuring delicate, high-temperature, or rotating objects, where attaching a sensor might alter the dynamics of the system or be outright impossible.

Another major advantage of LDV is its high precision [15]. LDV can measure displacements in the picometer range and velocities in the micrometer per second range. This level of precision is critical for applications that require detailed analysis of vibrational characteristics, such as in aerospace engineering or microelectromechanical systems (MEMS).

Furthermore, LDV systems can operate over a wide frequency range, from a few hertz to several megahertz [19], [20]. This wide operational range makes LDV suitable for various applications, from structural health monitoring to biomedical diagnostics. Additionally, the high spatial resolution of LDV allows for precise measurements at specific points on the surface, which is crucial for identifying localized defects or abnormalities in the material.

*3) Disadvantages of LDV:* Despite its numerous advantages, LDV also has some limitations. One of the primary drawbacks is the cost. LDV systems are generally more expensive than traditional contact-based sensors, which can be a significant barrier for some applications, particularly in cost-sensitive industries.

LDV measurements are also sensitive to the properties of the surface being measured. The quality of the measurement depends on the reflectivity and roughness of the surface. Highly reflective or very rough surfaces can introduce noise and reduce the accuracy of the measurements. Additionally, LDV systems can be affected by environmental factors such as vibrations, air turbulence, and temperature variations, which may require additional measures to mitigate these effects [19].

The complexity of LDV systems is another disadvantage. The setup and alignment of LDV systems can be complex and require skilled operators [20]. This complexity can increase the time and cost associated with using LDV for vibration measurements, especially in field applications where conditions may be less controlled than in a laboratory setting.

### C. Micro-electromechanical Systems (MEMS)

Micro-Electro-Mechanical Systems (MEMS) accelerometers are widely used for measuring acceleration and vibration due to their compact size, low power consumption, and high sensitivity. The following section introduces the principles behind MEMS accelerometers, their advantages, and disadvantages.

*1) Principles of MEMS Accelerometers:* MEMS accelerometers function based on various principles such as piezoresistive, piezoelectric, capacitive, tunnel, and resonant effects. The core working mechanism typically involves a suspended mass (proof mass) attached to a microfabricated structure. When subjected to acceleration, the inertial force causes displacement of the proof mass, which is detected by transducers and converted into an electrical signal. The capacitive MEMS accelerometer, one of the most common types, as shown in Fig. 4, measures the change in capacitance between the proof mass and fixed electrodes. This capacitance change is proportional to the acceleration experienced by the device.

The relationship between the displacement $x$ and acceleration $a$ can be expressed as

$$a = \frac{d^2x}{dt^2} \tag{7}$$

The change in capacitance $C$ is given by

$$\Delta C = \frac{\epsilon A}{d-x} - \frac{\epsilon A}{d+x} \tag{8}$$

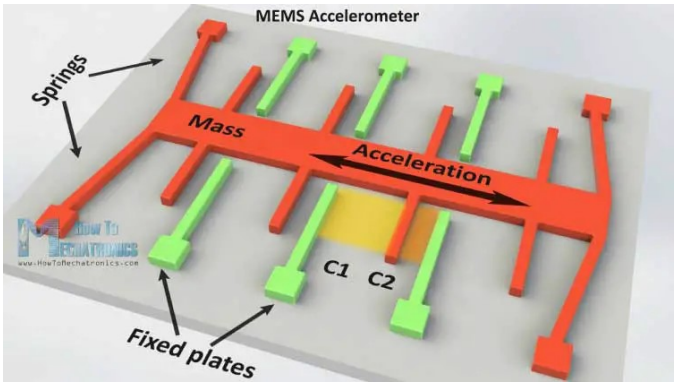


Fig. 4. The capacitive MEMS accelerometer, which measures the change in capacitance between the proof mass and fixed exlectrodes to get acceleration [22].

where $\epsilon$ is the permittivity of the material between the plates, $A$ is the area of the plates, $d$ is the initial separation between the plates, and $x$ is the displacement.

*2) Advantages of MEMS Accelerometers:* One of the primary advantages of MEMS accelerometers is their compact size and low power consumption [13], [14]. Due to their micro-scale dimensions and integration with semiconductor technology, MEMS accelerometers can be embedded into various devices without adding significant weight or bulk. This feature makes them ideal for portable and embedded systems, which require minimal power to operate efficiently.

Another significant advantage is their high sensitivity and precision. MEMS accelerometers can achieve high levels of sensitivity and precision through advanced fabrication techniques and sophisticated signal processing methods [14]. For instance, capacitive MEMS accelerometers offer excellent resolution and stability, making them suitable for applications requiring precise measurements.

Moreover, MEMS technology allows for mass production using standard semiconductor manufacturing processes, which reduces costs and enables widespread deployment [13]. The ability to produce MEMS accelerometers on a large scale at a low cost is a key factor driving their adoption in various industries.

Additionally, MEMS accelerometers are designed to withstand harsh environments, including high temperatures and shock. Their robustness and reliability [5] make them suitable for industrial and military applications where durability is crucial.

*3) Disadvantages of MEMS Accelerometers:* Despite their numerous advantages, MEMS accelerometers also have some limitations. One of the main drawbacks is their sensitivity to temperature variations [14]. Changes in temperature can affect the accuracy and stability of MEMS accelerometers, necessitating advanced packaging and temperature compensation techniques to mitigate these effects.

Another limitation is their relatively limited dynamic range compared to macroscopic accelerometers [5], [10]. This limitation can be a constraint in applications that require the measurement of high acceleration levels, such as in automotive crash testing or high-impact sports.

Furthermore, the small signals generated by MEMS accelerometers require complex signal processing and noise reduction techniques to ensure accurate measurements [10]. The need for sophisticated electronics can increase the overall system complexity and cost.

Lastly, variations in the microfabrication process can lead to inconsistencies in sensor performance. Each MEMS accelerometer may require individual calibration [13] and quality control to ensure they meet the required specifications, which can add to the production time and cost.

### D. Eddy Current Sensor

Eddy current sensors are non-contact devices that accurately measure the distance and displacement between a metal conductor and the sensor's probe, both statically and dynamically. They rely on the eddy current effect to determine relative positions with high linearity and resolution. These sensors are noted for their reliability, sensitivity, strong interference resistance, fast response times, and immunity to contaminants like oil and water. They are commonly used in large rotating machinery for continuous monitoring of parameters such as shaft displacement, vibration, and speed, aiding in the analysis of equipment condition and fault diagnosis, thus enhancing protective and preventive maintenance.

*1) Principles of Eddy Current Sensor:* The working principle of eddy current sensor system is eddy current effect, which belongs to an inductive measurement principle, as shown in Fig. 5. Eddy current effects are derived from the energy of the oscillating circuit. Eddy currents need to be formed in a conductive material. Introduce an alternating current to the coil in the sensor probe to form a magnetic field around the probe coil. When a massive metal conductor is placed in a changing magnetic field or moves with a cutting magnetic line of force in the magnetic field (it is irrelevant to whether the metal is massive, and there is no eddy current when cutting the unchanged magnetic field), an inductive current in the form of vortex will be generated in the conductor. This current is called eddy current, and the above phenomenon is called eddy current effect [23].

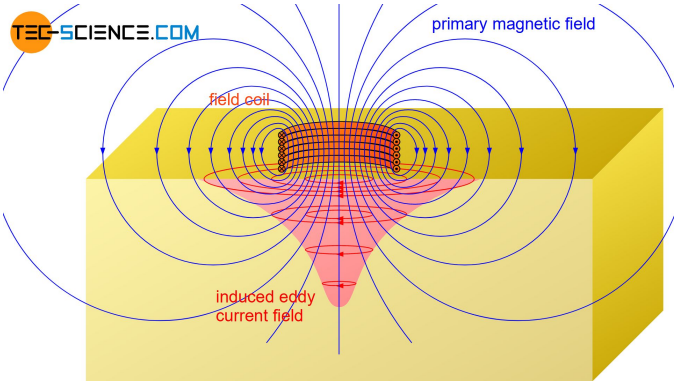


Fig. 5. The eddy current sensor is based of eddy current effect, which belongs to an inductive measurement principle [24].

Based on Lenz's law, the magnetic field direction of the eddy current is exactly opposite to the coil magnetic field,

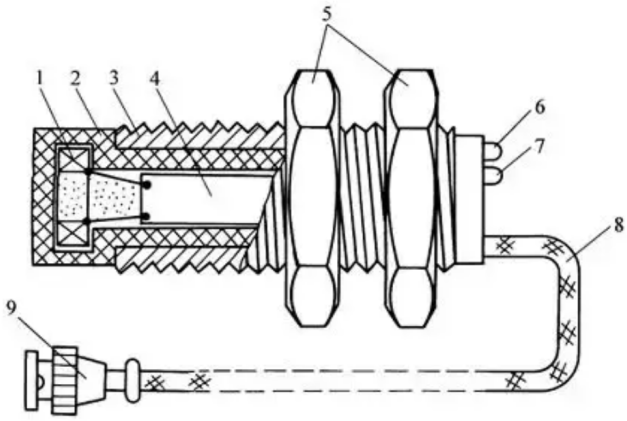


Fig. 6. The structure of Eddy Current Sensor: 1 - Eddy coil 2 - Probe housing 3 - Position adjustment thread on housing 4 - PCB 5 - Holding nut 6 - Power indicator 7 - Threshold indicator 8 - Output shielded cable 9 - Cable plug [25].

which changes the impedance value of the coil in the probe. This change is related to the magnetic conductivity of the metal body, conductivity, coil geometry, geometry, current frequency, and distance from the head coil to the surface of the metal conductor. Generally, it is assumed that the metal conductor material is uniform and the performance is linear and isotropic, then the physical properties of the coil and the metal conductor system can be described by the conductivity of the metal conductor, the magnetic conductivity $\xi$, the size factor $\tau$, the distance D between the head body coil and the metal conductor surface, the current intensity I and the frequency $\omega$ parameters. Then the characteristic impedance of coil can be Z=F ($\tau$ , $\xi$. D, I, $\omega$) function. When the sensor probe is connected to the controller, the controller can obtain the variation of voltage value from the sensor probe, and calculate the corresponding distance value based on this. Eddy current measurement principle can measure all conductive materials.

Since eddy current can penetrate the insulator, even the metal material covered with insulator can be used as the object to be measured of eddy current sensor. The unique coil winding design allows the sensor to operate in high temperature measurement environments while providing a compact shape.

*2) Advantages of Eddy Current Sensor:* Eddy current sensor is a kind of non-contact linear measuring tool, which can statically and dynamically measure the distance between the metal conductor to be measured and the probe surface with non-contact, high linearity and high resolution [25].

*3) Disadvantages of Eddy Current Sensor:* When the sensor characteristics and the conductivity of the measured body exist at the same time, the magnetic effect reacts on the eddy current effect to weaken the eddy current effect, that is, the sensitivity of the sensor is reduced.

Irregular surface of the object to be measured will bring additional error to the actual measurement, so the surface of the object to be measured shall be flat and smooth, and free from such defects as bulge, hole, notch and groove. Generally, the roughness of the surface to be measured for vibration measurement shall be between 0.4um and 0.8um; For

displacement measurement, the measured surface roughness shall be between 0.4um and 1.6um.

Eddy current effect is mainly concentrated on the surface of the object to be measured. If residual magnetic effect is formed during processing, and non-uniform quenching, hardness, metallographic structure and crystal structure will affect the characteristics of the sensor. During the vibration measurement, if the residual magnetic effect on the surface of the measured body is too large, the measurement waveform will be distorted [25].

### *E. GRID method*

The grid method for measuring the vibration of nuclear fuel rods involves engraving or transferring a regular grid of lines onto the surface of the rods. The idea is to detect the deformation of these grid lines when the rods are vibrating. The grid lines are flexed as the fuel rods buzz, which gives rise to a fringe pattern. Using a camera to capture the initial and deformed states of the grid, one can then process the images to extract phase maps which are used to determine how each of the rods is displaced or strained. These phase maps are subtract and derive the strain induced by the vibration. This technique permits to accurately measure large displacement and strain over a wide area as a consequence of the low frequencies of the grid lines compared to traditional techniques [9].

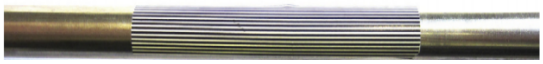

Fig. 7. Engraved grid pattern on fuel rod.

By examine a fringe pattern generated by one of the researcher measuring techniques mentioned. The light intensity, denoted as s, for each pixel of the camera that records the fringes may be expressed in the following manner:

$$s(x) = A[1 + \gamma \cdot \text{frgn}(2\pi f x + \phi)] \tag{9}$$

where $A$ represents the amplitude, $\gamma$ represents the contrast, frng is a $2\pi$ periodic function, $f$ represents the frequency of the carrier, which is defined by the inverse of its pitch $p$, $x$ represents the coordinate that is transverse to the line array, and $\phi$ represents the carrier phase modulation, which is related to the in-plane displacement $u$ through the following equation:

$$\Delta\phi = -\frac{2\pi}{p} \times u \tag{10}$$

$\Delta\phi$ is used to denote the phase variation in this context. In most cases, the following approach may be used to determine the strain from the displacement: Beginning with the calculation of the initial phase distribution and the final phase distribution, the fringes are used. One approach of accomplishing this goal is by use spatial or temporal phase shifting techniques. It is feasible to find out both the phase difference and the displacement since they are directly connected. Reason being, there is a direct line of communication between the two. Filtering the displacement field spatially is what this procedure entails. The numerical differentiation of this filtered displacement field is an inherent consequence of time passes [26].

Fig. 8. Grid system setup.

The advantages of GRID method for nuclear fuel rod vibration measurements provides the following benefits; The GRID method provides high accuracy, engraving on the surfaces of the rod with fine deformation geometric data, The GRID method with dense surface markers can be employed to measure the displacement and strain with a wide-surface-area precision without vertical interception for the rod, The GRID method is a viable and useful vibration measurement tool in power plant nuclear industry, often exposed to high temperature and tri-axial impact loads, when displacement and strength measurement calls for the expected precision, The GRID method is non-intrusive, portable, flexible, and provides detailed observation of deformation contour of the grid lines applied to the rod surfaces. But of course, that requires an installation to move light in a grid above the system, and the system is sensitive to environmental conditions, such as lighting and temperature. One major drawback is that, like the video-based tracking that was known to have accuracy issues, the method requires advanced image processing for data extraction, and tabletop optical equipment requires regular maintenance and calibration that can be time consuming and expensive.

### *F. Comparison in FIV Measurement*

In literature [5], a FIV measurement system was constructed to discuss the impact of technologies such as LDV, GRID, FBG, and MEMS on rod dynamics, specifically the changes in vibration modes they induce. It also compared the signal-to-noise ratio (SNR) and the sensors' ability to respond to low-frequency and low-amplitude signals. The conclusion was that, for this experimental setup, optical technologies and MEMS-type accelerometers demonstrated superior performance. The relevant experimental results are presented in Table I, where R2 Quality Factor indicates the goodness of fit of the sine wave to the measured data. It can be observed that LDV indeed has the highest R2 Quality Factor and SNR. Additionally, it features non-contact measurement, making it an excellent tool for FIV measurements. However, the non-contact measurement achieved through optical methods has its inherent limitations, such as the inability to measure the vibration of the inner rod, which necessitates the assistance of additional

sensors. Following LDV, MEMS sensors exhibit the highest SNR. Although they may slightly affect the rod's modes, their overall accuracy remains sufficiently high. Furthermore, their small size and contact measurement capability facilitate the measurement of inner rod vibrations.

## III. Problem Statement

In a nuclear power plant, when the cooling fluid flows through the bundle of rods, it can excite vibrations in the bundle and the outer wall, which is called flow-induced vibration (FIV) [27]. The vibration frequency of FIV can vary significantly depending on the flow velocity and specific conditions. According to the studies, the following key points are observed regarding FIV frequencies. Generally, FIV frequencies are low, typically below 200 Hz in many observed cases, which is called low frequency vibrations (LFV). However, Under certain conditions, such as higher flow velocities, high frequency vibrations (HFV) can be observed. For instance, a strong high frequency vibration of about 2 kHz was detected. Additionally, high frequency vibrations around 3 kHz were noted when the flow velocity reached certain thresholds, such as 3.88 m/s and above. In addition, resonance can occur at specific flow velocities, leading to stronger vibrations. For example, a strong resonance frequency was observed at 6567 Hz when the flow velocity was 7.35 m/s [4].

In order to study FIV in nuclear power plants [1], a simplified $3 \times 3$ rod bundle model is constructed, as shown in Fig. 9. The stainless steel rods are confined by a rectangular

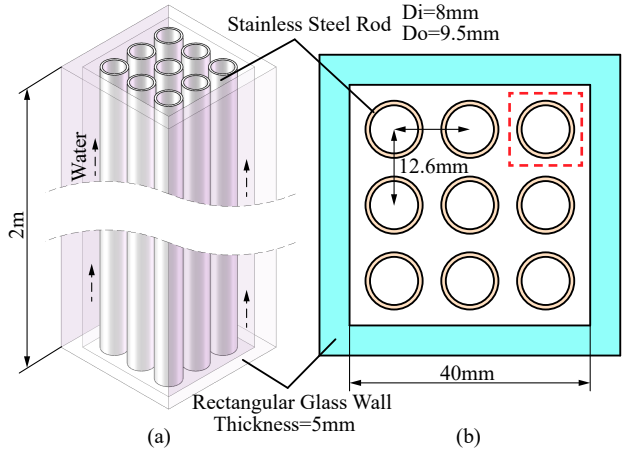


Fig. 9. A $3 \times 3$ rod bundle model that simplifies cooling rods in nuclear power plants. The stainless steel rods are confined by a rectangular glass wall with a length of 2m. (a) The 3D view of the $3 \times 3$ rod bundle model. Water with a speed of 1 to 8 m/s flows from the bottom up between the glass wall and the rods. (b) Top view and key dimensions of the model.

glass wall with a length of 2m, whose inside side length is 40mm and thickness is 5mm. The 9 rods are evenly distributed, the distance between them is 12.6mm, and their inner diameter is 8mm and the outer diameter is 9.5mm. To simplify matters, our environment is set to room temperature (25°C) and normal atmospheric pressure (0.1MPa). Water flows between the glass wall and the rod bundle at a speed of 1 to 8 m/s, which might cause the above three kinds of vibrations. We need to measure the vibration on the glass wall and each rod, of which the vibration on the corner rod (shown in the red box in Fig. 9) requires special attention.

Due to the small distance between the rods, small size of the rods and the interference of the flowing liquid, the type, size and layout of the sensors are critical. Thus, we design the hardware system of rod and glass wall vibration measurement, and outline the test process of data processing, so that this system can be applied to the measurement of real systems. The following sections will introduce vibration measurement system design and test procedure design in detail.

## IV. Measurement System Design

In our quest to accurately measure the vibrations within the central section of a $3 \times 3$ fuel rod array, this research has meticulously integrated two state-of-the-art measurement technologies: MEMS accelerometers and Laser Doppler Vibrometers (LDV). Due to the small size, low cost and high precision of MEMS, as well as the characteristics of contact measurement, it is suitable for distributed vibration measurement of the rods and the glass wall, whether they are inside or outside. LDV has the advantages of non-contact measurement and ultra-high precision [5], which is very suitable for measuring the vibration of the corner rod, but because it is based on light, it cannot be used to measure the vibration of the internal rod. LDV can also be used to measure the vibrations of glass walls by simply attaching reflective tape to the vibrating wall. Thus, we use a MEMS array to measure the vibration of the glass wall and all rods, and use LDV to provide the precise vibration of the corner rod and the wall. Since MEMS itself is sufficient to measure vibration, the existence of LDV is more for improving accuracy, but due to its high cost, the use of LDV is optional.

### A. System Configuration

The architecture of the measurement system and the position of each sensor are shown in Fig. 10. The glass wall and each rod are equipped with multiple MEMS accelerometers, with each layer of every rod uniformly distributed with three sensors, and each layer of the glass wall having four. This distribution can have multiple layers along the direction of the rods. The distributed sensor layout on each layer allows us to accurately measure vibrations at multiple points and, with the help of multi-sensor data fusion technology, achieve error compensation. The multi-layer structure facilitates the exploration of vibration distribution along the rods. An LDV is mounted on the outside to measure the vibrations of the corner rods, and its direction can be changed to measure the vibrations of the rods in two directions. With the aid of reflective tape, LDV is also used for precise measurement of glass wall vibrations. Due to the high price, the use of the LDV is optional.

### B. Sensor Model Selection

The MEMS accelerometers, specifically the IIS2DH model (STMicroelectronics N.V., Switzerland), as shown in

TABLE I
COMPARISON IN ROD VIBRATION MEASUREMENT [5]

| Sensor | Original 1st Mode (Hz) | Original 2nd Mode (Hz) | Δ1st Mode (Hz) | Δ2nd Mode (Hz) | R2 Quality Factor | SNR (dB) | Notes |
|---|---|---|---|---|---|---|---|
| LDV | 8.45 | 29.42 | 0.09 | 0.04 | 99.9% | 68.5 dB | Non-contact, high performance |
| GRID | 8.44 | 28.23 | 0.76 | 1.70 | 96.2% | 45.5 dB | Non-contact, affected by stiffness |
| FBG | 8.42 | 28.00 | 0.15 | 1.88 | 92%-99.5% | 37.6-46.9 dB | Contact, good performance |
| MEMS | 8.44 | 28.23 | 0.88 | 2.29 | 99.7% | 65.4 dB | Contact, high performance |
| Eddy Current | - | - | - | - | - | - | Non-contact |

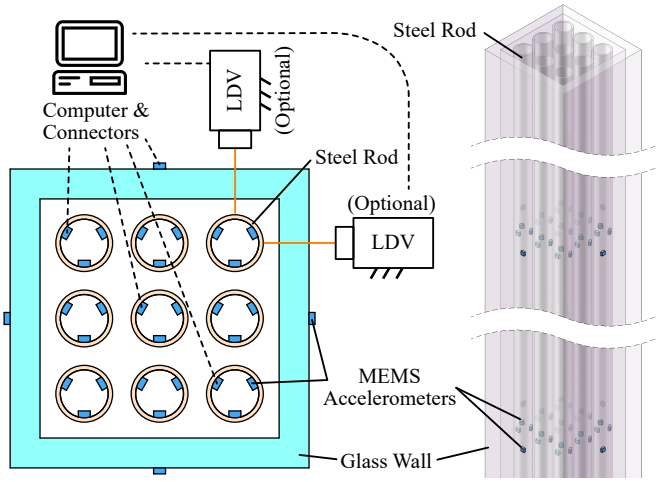


Fig. 10. Sensor positions and measurement system configuration. Multiple MEMS accelerometers are distributed on the glass wall and each rod, of which 3 are evenly distributed on each layer of each rod, and 2 are on each layer of the glass wall. This distribution has multiple layers along the rod direction. Optionally, the 2D vibrations of the outer rods can be synchronously measured by the LDVs.


(a) IIS2DH (b) OFV5000

Fig. 11. MEMS accelerometer model IIS2DH and LDV model OFV5000.

Fig. 11(a), have been selected for their small size, exceptional sensitivity and wide-ranging frequency response capabilities. Table II displays the main parameters of the IIS2DH, which has dimensions of only $2\times2\times1$ mm, small enough to be placed inside the rod. Additionally, its adjustable measurement range and high sampling frequency enable us to better measure the vibrations of the rod and glass wall.

The LDV, OFV5000 (Polytec GmbH, Germany), as shown in Fig. 11(b), is tasked with gauging the vibration of the outer rods. The main parameters of OFV5000 is shown in Table II. Its non-contact measurement approach is a significant advantage, allowing it to precisely record vibration data without any disruption to the flow field, which is indispensable for examining the effects of fluid dynamics on the rod bundle's vibrations. The LDV contributes to the study by delivering accurate and high-resolution vibration velocity measurements, facilitating an in-depth analysis of the rod bundle's dynamic reactions.

To facilitate installation, we arranged a two-layer sensor array as shown in Fig. 10, requiring a total of 62 MEMS accelerometers. Since the LDV is placed externally and can be moved around, only one LDV is needed to meet the requirements. Consequently, depending on whether the LDV is used, the budget for sensor procurement is approximately $197 (about CNY 1,450) or $25,197 (about CNY 182,500).

### C. Installation of Sensors

The sensors on the glass wall are easy to install, requiring only glue or double-sided tape for attachment. However, installing the MEMS accelerometers inside the rod and the external LDV requires certain skills.

To prevent the vibrations of the rods and glass wall from affecting the LDV itself, the LDV needs to be securely fixed and isolated from the system being measured. One feasible solution is to mount it on an optical table, which not only helps stabilize the LDV but also facilitates moving the LDV from one position to another.

Fixing MEMS accelerometers inside the rod generally requires specialized adhesive. However, since the bottom of the MEMS accelerometers is flat, additional brackets are necessary to ensure adhesive strength when attaching them to a curved surface. These brackets, as shown in Fig. 12(b), are adhered to the back of the sensors to avoid affecting the sensor pins. The sensor pins are soldered with wires that extend to the side, facilitating their routing out of the rod. We use a flexible flat cable, which features a slim profile and integrated design. This helps reduce the overall size of the MEMS accelerometer and makes cable management easier.

The installation process for the MEMS accelerometer requires the use of installation tool, as shown in Fig. 12(a). First, apply low-viscosity glue to the installation tool and attach the MEMS accelerometer. Insert it into the correct position within the rod, then press the MEMS accelerometer against the inner wall of the rod. After the high-viscosity glue dries, gently break the bond of the low-viscosity glue to separate the installation tool from the MEMS accelerometer.

TABLE II
MAIN PARAMETERS OF MEMS ACCELEROMETER IIS2DH AND LDV OFV5000

| Model | Size | Measurement range | Resolution | Sample rates | Price |
|---|---|---|---|---|---|
| IIS2DH | $2 \times 2 \times 1$ mm | Acceleration: $\pm 2g/\pm 4g/\pm 8g/\pm 16g$ | $0.98mg/1.95mg/3.91mg/11.72mg$ | 1 Hz to 5.3 kHz | $3.18 |
| OFV5000 | – | Velocity: up to 10 m/s | 0.02 $\mu$m/s (1 Hz) | 1 Hz to 24 MHz | Typically $25,000 |

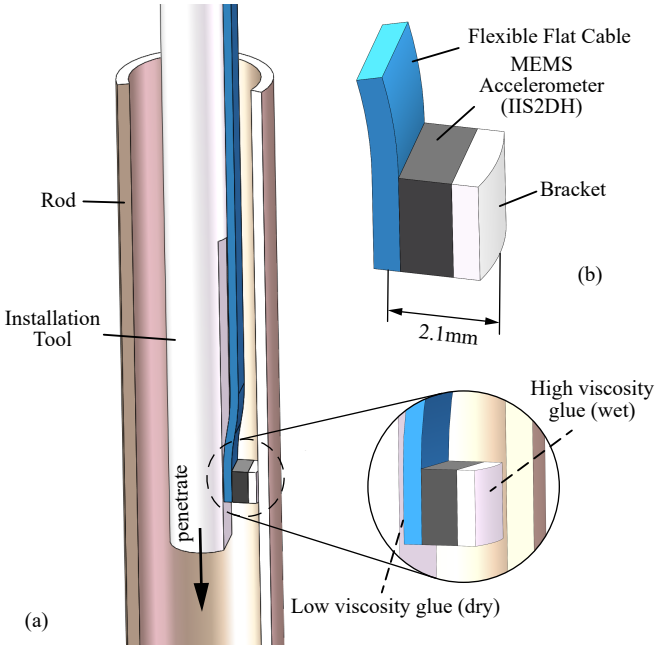


Fig. 12. The processing method and installation procedure of MEMS accelerometers. (a) Install the MEMS accelerometer using the installation tool. (b) The MEMS accelerometer is clamped between the bracket and the Flexible Flat Cable.

Finally, remove the installation tool from the rod. Each MEMS accelerometer must be installed individually rather than all at once, due to the rod's inner diameter of only 8 mm and the complex structure that is difficult to process. To ensure precise installation of each sensor, the installation tool needs to be marked. This will ensure that the MEMS accelerometer is attached at the same position on the installation tool each time and that the insertion depth into the rod remains consistent.

## V. TEST PROCEDURE

### A. Calibration

In this study, we ensure the accuracy of vibration measurements through precise calibration of MEMS accelerometers. The calibration process involves using a vibration exciter, function generator, power amplifier, signal analyzer, and a reference accelerometer, all conducted under controlled environmental conditions. The MEMS accelerometer is securely mounted on a support structure and powered by an Arduino micro-controller for sweep calibration across a set range of frequencies and amplitudes.

Utilizing a JX-3B (Beijing Instrument Industry Co., Ltd., China) vibration sensor calibrator, valued at CNY 12,000, we generate sinusoidal signals with frequencies ranging from 10Hz to 1280 Hz, with an accuracy of ±0.01%. By adjusting the potentiometer, signals with peak acceleration of 100m/s², RMS velocity of 170mm/s, and peak-to-peak displacement of 2mm are outputted. The sensitivity and zero point of the MEMS accelerometers are adjusted by comparing the output signals with theoretical values to ensure the accuracy of the measurements.

$$v = \frac{a}{2\pi f} \tag{11}$$

Fig. 13. JX-3B Vibration Exciter from Beijing Instrument Industry Co.,Ltd.,China.

The calibration of the LDV is not necessary, yet we address the laser beam transmission process, particularly when the measured object is immersed in water. The LDV emits a laser beam that travels through air and water, reflecting off the vibrating object's surface before returning to the LDV. We modify the measured vibration results based on the refractivity of water to maintain accuracy, as shown in the equation provided.

It's important to note that at an angle of incidence less than 8 degrees [28], the velocity measured by the LDV deviates from the actual motion velocity of the object by less than 1%. This precision is critical for our experiments and ensures the reliability of our measurements.

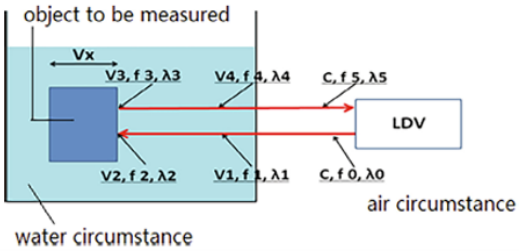


Fig. 14. Laser beam transmission process of vibration measurement by the LDV for a measured object immersed in water [23].

$$f_5 - f_0 = \frac{2nv_x}{\lambda_0} \tag{12}$$

$$v_x = \frac{v_{x,m}}{n} \tag{13}$$

Another co-calibration process of MEMS accelerometers using our LDV, for enhanced precision in vibration measurements. We've established an experimental setup where both MEMS and LDV measure a point on a simply supported beam concurrently. This allows us to use the LDV's high-precision velocity readings to calibrate the MEMS accelerometers accurately.

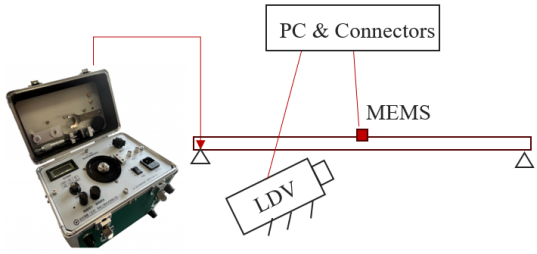


Fig. 15. Co-Calibration System of MEMS and LDV.

Our procedure involves collecting sequential acceleration data from the MEMS sensors, which we then convert into velocity for direct comparison with the LDV's measurements. The synchronization of the LDV with the MEMS ensures that we capture simultaneous readings, crucial for an accurate co-calibration. To validate this calibration method, we've crafted a comprehensive table documenting the measurements at specific frequencies—160 Hz, 320 Hz, 640 Hz, and 1280 Hz [28]. For each frequency, we have set acceleration and velocity values. The table records the acceleration measured by the MEMS, the velocity calculated from it, and compares this velocity with that measured by the LDV. This comparison allows us to assess and adjust the MEMS accelerometers against the LDV's benchmark, ensuring our measurements are precise and reliable.

TABLE III
CALIBRATION TEST DATA TABLE

| Exciter | | | MEMS | | | | LDV | |
|---|---|---|---|---|---|---|---|---|
| $f$ | $a$ | $v$ | $a$ | $e$ | $v$ | $e$ | $v$ | $e$ |
| 160 | 2.0 | 1.989 | | | | | | |
| 320 | 2.0 | 0.995 | | | | | | |
| 640 | 2.0 | 0.497 | | | | | | |
| 1280 | 2.0 | 0.249 | | | | | | |

## B. Experimental Procedure

The experimental procedure of this study aims to simulate the operating conditions in a nuclear reactor and measure the resulting flow-induced vibrations. The experiment first takes place under non-water conditions to assess the structural vibration characteristics. Subsequently, deionized water is added to the container, and the flow rate is gradually increased to simulate different coolant flow conditions. At each flow rate, at least 5 minutes of vibration data are recorded to ensure the statistical reliability of the data. To be specific, the whole procedure is as follows:

1) Before the experiment begins, all system valves are opened to thoroughly flush the entire loop system. The sealing conditions of all valves, nuts, and thermocouples are inspected to ensure there are no leaks. After confirmation, deionized water is added to the tank to prepare for the experiment.
2) The differential pressure sensor is calibrated to zero. If necessary, residual gases are expelled and the sensor is finely adjusted to zero. Additionally, the signal input and output of the data acquisition system are verified for normal operation.
3) To install MEMS accelerometers internally, mark positions on the rod's inner wall. Employ custom brackets adhered with high-strength adhesive, fitting MEMS flat underside, and solder wires extending laterally with a flexible cable. Use a specialized tool: apply low-viscosity glue, insert the accelerometer, and after adhesive sets, detach tool for a firm installation. Each unit is individually placed with indexing for precision.
4) The LDV is used to measure the vibrations of the surrounding eight rods, synchronized with measurements taken by the MEMS accelerometers, ensuring consistency and accuracy of the data. Meanwhile, we could acquire the vibration of the middle rod.
5) The vibrations of the glass container are measured using MEMS accelerometers to assess the dynamic response of the container under fluid flow.
6) The experimental section is fixed onto a dedicated support frame and connected to the loop system via hoses.
7) The laser head of the vibrometer is mounted on a tripod and connected to controllers and an oscilloscope. After at least 30 minutes of warm-up, the laser head is aimed at the measurement point, and the focus is adjusted until the signal is stable, with parameters set on the controller.
8) The main pump is started and adjusted to the predetermined flow rate to maintain system stability. Within the flow velocity range of 1-8 m/s, measurements are taken repeatedly at each measurement point, recording vibration data and relevant parameters.
9) After completing all flow conditions, the LDV is adjusted to the next measurement point, and the steps are repeated until all data is collected. After the experiment is concluded, the data is comprehensively processed and analyzed.
10) Throughout the experimental process, any anomalies should be immediately noted, and the experiment should be paused if necessary, resuming only after issues are resolved.

## C. Data Acquisition

In this study, we implemented a unique setup of MEMS accelerometers arranged at 120-degree intervals around a circle to comprehensively capture the vibration characteristics of a fuel rod bundle and its environment. The MEMS accelerometers were connected to the data acquisition system via IIC (Inter-Integrated Circuit) or SPI (Serial Peripheral Interface)

communication protocols, which support high-speed, low-latency data transfer and facilitate communication with multiple sensors. The acquisition modules were set to continuously record data at a fixed sampling rate, and hardware filters were used to eliminate noise, enhancing data quality and accuracy. Further software algorithms were applied for data processing.

Simultaneously, the LDV system, equipped with a dedicated data collector, recorded vibration velocity data at a high sampling rate. Its non-contact nature allowed for precise measurements without disrupting the flow field, and the system was carefully aligned to synchronize with the MEMS accelerometers' sampling rates. A central data acquisition system (DAQ) was utilized to synchronize and coordinate the data streams from both types of sensors, featuring high-precision clock synchronization to ensure the temporal consistency of data collection and supporting real-time monitoring capabilities.

After collection, the data were stored in high-speed data recorders and underwent preprocessing, which included denoising, filtering, and normalization, using professional data acquisition and analysis software designed for data visualization and further processing. In the preprocessing phase, high-pass filtering was critical to removing potential zero-bias and reducing integration drift from the MEMS accelerometer data, thus preparing it for accurate frequency analysis using Fast Fourier Transform (FFT) techniques.

$$H(f) = \frac{f}{f + f_c} \tag{14}$$

Here, $H(f)$ represents the transfer function of the high-pass filter, $f$ denotes the frequency of the signal, and $f_c$ is the cutoff frequency, which defines the threshold frequency at which the filter significantly attenuates the lower frequency components of the signal.

$$y[n] = \alpha\left(x[n] - 2x[n-1] + x[n-2]\right) + 2y[n-1] - y[n-2] \tag{15}$$

In the difference equation for a second-order high-pass filter, $y[n]$ represents the current output sample of the filter. The terms $x[n]$, $x[n-1]$, and $x[n-2]$ denote the current, previous, and two-time previous input samples, respectively. Similarly, $y[n-1]$ and $y[n-2]$ refer to the previous and two-time previous output samples. The coefficient $\alpha$, calculated based on the cutoff frequency $f_c$, adjusts the frequency response of the filter, affecting how the filter attenuates the lower frequency components of the input signal.

To integrate the multi-directional data from the MEMS sensors more effectively and to potentially combine them with the LDV data for deeper analysis, a Kalman filter could be employed. This advanced filtering technique would allow for the optimal estimation of the system's state by processing the noise and inaccuracies inherent in data from diverse sources.

Once in the global coordinate system, the acceleration data from the three directions were recombined using vector synthesis. This step involved either simple vector addition or the application of more sophisticated data fusion algorithms, such as the Kalman filter, to integrate data from all three directions into a single comprehensive acceleration vector that describes the system dynamics, with the following key mathematical models and equations:

In our setup, MEMS accelerometers are strategically positioned at 120-degree intervals around the fuel rods and the glass wall, with configurations of 3 sensors for rods at angles of 30°, 150°, and 270°, and 4 sensors for the glass wall at 0°, 90°, 180°, and 270°. This arrangement ensures a comprehensive capture of the vibration characteristics.

The MEMS data is transmitted through established data protocols, leveraging the high-speed, low-latency capabilities of IIC or SPI communication. This setup facilitates seamless communication with multiple sensors and allows for the continuous recording of data at a fixed sampling rate. Our data processing workflow involves several key steps. Initially, we apply coordinate transformations to align the data from various sensors. These transformations are computed using rotation matrices, which adjust the data into a common reference frame.

Following the coordinate alignment, we engage in data fusion techniques. We utilize methods such as averaging or Kalman filtering to integrate data from different sensors into a coherent set.

To utilize Kalman filtering [17] for fusing multiple accelerometer readings, we establish a state-space model consisting of a state vector that includes position, velocity, and acceleration. The state equation models the evolution of these states over time, while the measurement equation relates the accelerometer measurements to the state vector. In this model, the state transition matrix, control input matrix, and measurement matrix are defined to capture the dynamics and observations of the system. By processing the acceleration data from multiple sensors and applying the Kalman filter equations, we can accurately estimate the system's position, velocity, and acceleration, effectively compensating for noise and discrepancies in the sensor readings.

Predicted state estimate:

$$\hat{x}k|k-1 = F_k\hat{x}k-1|k-1 \tag{16}$$

Predicted error covariance:

$$P_{k|k-1} = F_k P_{k-1|k-1} F_k^T + Q_k \tag{17}$$

Kalman gain computation:

$$K_k = P_{k|k-1} H_k^T (H_k P_{k|k-1} H_k^T + R_k)^{-1} \tag{18}$$

Updated state estimate:

$$\hat{x}k|k = \hat{x}k|k-1 + K_k(z_k - H_k\hat{x}_{k|k-1}) \tag{19}$$

Updated error covariance:

$$P_{k|k} = (I - K_k H_k) P_{k|k-1} \tag{20}$$

After fusion, we focus on noise reduction. While it's important to retain useful information within the data, we apply low-pass filtering to minimize the effects of noise and prepare the data for further analysis.

We finally conduct a Fourier transform on the processed data to extract the frequency components. This continuous-time Fourier transform reveals the underlying frequencies present in

the vibration data, providing valuable insights into the system's behavior.

Ensuring the security and integrity of the experimental data was paramount, and thus a multi-tier backup strategy was adopted. Data were immediately duplicated to multiple storage devices upon collection and backed up on secure servers, providing a robust defense against data loss and ensuring data integrity for comprehensive analysis and long-term study.

This approach ensures that every aspect of data handling, from initial collection through to advanced analysis, is carefully managed to provide a thorough understanding of the system's dynamics and to support ongoing monitoring and maintenance strategies.

If ldv is used, our objective is to extract the frequency components of these vibrations, and to achieve this, we employ two primary steps: low-pass filtering and continuous-time Fourier transform. To be specific:

Corner rods:There are 4 corner rods, each with the capacity for two measurements, providing us with a robust dataset from these critical junction points.

Edge rods:Similarly, there are 4 edge rods, with one measurement possible for each, contributing valuable data from the periphery of the bundle.

Inner rod:The central rod, which cannot be directly measured by the LDV due to accessibility constraints, is instead monitored using MEMS accelerometers. This strategic measurement approach ensures that we capture a comprehensive vibration profile of the rod bundle, leveraging the high precision of the LDV for the outer rods and the versatility of MEMS for the inner rod.

### *D. Data Processing and Analysis*

Data processing and analysis are important steps in this study to extract useful information and verify the results of the experiment.

During the data processing, particular attention is paid to vibration frequency, amplitude, and phase information, which are crucial for understanding the dynamic behavior of the rod bundle. By comparing the vibration data under different flow rates, the potential impact of flow-induced vibrations on the integrity of the fuel rods can be assessed. Additionally, statistical methods, such as analysis of variance and correlation analysis, are used to evaluate the reliability and repeatability of the measurement results.

Laser Doppler data processing involves several crucial steps to analyze and interpret the velocity data collected from fluid flows. The process begins with analyzing the stochastic sampled velocity data, which includes deriving sampling statistics such as the sampling interval distribution and the mean particle and validation rate. As Fig. 16 shows the LDV siganl processing in time domain. Next, velocity statistics are derived,

Fig. 16. Velocity acquired by LDV in time domain after signal processing.

including the mean velocity, velocity variance, auto-correlation function, correlation coefficient, structure functions, and power spectral density. These statistics provide insights into the central tendency, dispersion, and temporal correlation of the velocity data, as well as advanced turbulent characteristics.

Finally, characteristic flow parameters and two-point or two-component statistics are calculated. This involves determining the integral time or length scale, Taylor time or length scale, dissipation rate, cross-correlation function, correlation coefficient, and cross-spectral density function. These steps offer a comprehensive understanding of the fluid flow's statistical and physical properties. After carrying out data processing like Continuous Time Fourier Transform and get data in frequency domain as Fig. 17 shows. We are able to further understand the frequency characteristics of the vibrations in measured objects. The RMS value of the vibrations is calculated to assess the vibration intensity and is compared with theoretical models and expected results.

Fig. 17. Velocity acquired by LDV in frequency domain after data processing.

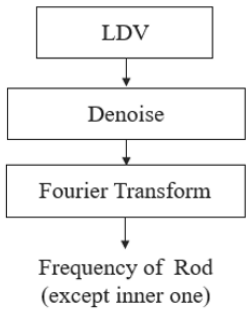


Fig. 18. LDV data processing flow chart.

The MEMS data processing is like Fig. 20 shows. Firstly, collect measurement values from all available sensors installed at different angles and places. Then, during the initial calibration period, estimate and compensate for the systematic error of each sensor. Then use the transformation matrix to transform the measured acceleration, angular velocity, and magnetic field vectors from the sensor coordinate system to the volumetric coordinate system. Then take the average of all measured values and pass it to the directional filter to process the signal and estimate its direction. Incorporate this information into trajectory recovery filters with various external signals to stabilize calculations. Similarly, Fourier Transform will be taken to get frequency characteristics of vibrations in both rods and wall.

### *E. Measurement Error Sources*

*1) LDV error sources:* The source of errors for laser measurement systems like LDV include Laser Doppler frequency broadening, interference of Gaussian beams, affected by the measuring medium and medium boundaries and installation error [29].

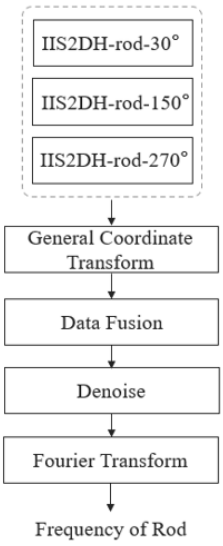


Fig. 19. MEMS data processing of rods flow chart.

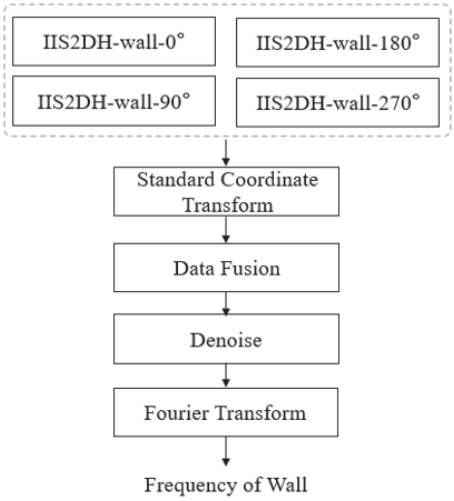


Fig. 20. MEMS data processing of glass wall flow chart.

For Laser Doppler frequency broadening, in an ideal scenario, when the laser measurement beam is directly incident on the surface of the target object, the detector receives a given fixed Doppler beat frequency. However, in the actual measurement process, the Doppler beat frequency we obtain is not a fixed value, but there is an inevitable Doppler signal broadening. The main reasons for laser Doppler spectrum broadening are finite time crossing widening, velocity gradient broadening and detector aperture broadening.

As for interference of Gaussian beams. Usually, when conducting theoretical analysis and calculations, light waves are considered as planar beams. Therefore, it is believed that the interference fringes formed in the measurement body are parallel fringes of equal width, and based on this, the Doppler measurement signal is obtained. However,the light coming out of the laser is not a parallel beam, but a Gaussian beam. Obviously,the interference fringes formed in the measurement body are no longer parallel fringes of equal width, and the angle between the two light sources decreases along the z-axis. The n-order fringes formed at the intersection of Gaussian beams can be expressed by the following formula:

$$X_n = \frac{n\lambda}{2\sin\theta} - \frac{n^3\lambda^5}{16\pi^2\omega_0^4\sin^3\theta} \tag{21}$$

The interference fringe is as Fig. 21 shows, and the interval can be expressed as:

$$\Delta X = X_n - X_{n-1}\frac{\lambda}{2\sin\theta} - (3n^2 - 3n + 1)\frac{\lambda^5}{16\pi^2\omega_0^4\sin^3\theta} \tag{22}$$

Where $n$ denotes the order of fringes; $\theta$ denotes the angle between the optical axes of two beams; $\lambda$ denotes the wavelength of the laser; $\omega_0$ denotes the diameter of the waist spot of the Gaussian beam.

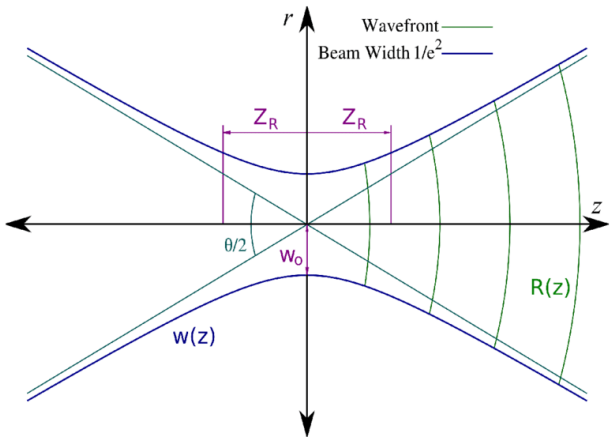


Fig. 21. The phenomenon of Gaussian beam interference [30].

As for different measurement media. When light is transmitted in different media, its propagation speed is different, but it does not cause the change of transmission frequency $f$, but the wavelength $C$ of light is different due to different media. However, when the laser beam is used to measure through several different media, due to refraction, the direction of the beam is deflected, which brings a lot of inconvenience and trouble to the measurement.When the experimental beam passes through a flat or circular window, it will deflect the beam and cause the position change of the measuring point.

As for installation error, when using laser Doppler technology to measure solid surfaces, there are still installation errors. Generally speaking, the angular bisector of two measuring beams coincides with the surface normal of the object being measured. However, in actual measurements, it is impossible to achieve complete overlap, which inevitably brings errors to the measurement results. When laser Doppler technology is used to measure the solid surface, there are still installation errors. Generally speaking, the angular bisector of the two measuring beams coincides with the surface normal of the measured object. However, in the actual measurement, it is impossible to achieve complete coincidence, which will inevitably bring errors to the measurement results. When measuring large diameter with laser Doppler technology, the

angular bisector of the two incident rays does not coincide with the normal of the measured surface due to the installation of the instrument.

*2) MEMS error sources:* The main sources of error in MEMS include static and dynamic bias, intrinsic noise, scale factor error, quadrature axis and the instability of zero bias [**?**].

For the bias, theoretically, the three-axis output is $\{0, 0, 0\}$ in the static state, but in fact, the output has a small offset, which is the static component of zero offset (also known as fixed zero offset). Of course, there is a dynamic component of zero bias. Dynamic bias is not a parameter. It will drift slowly and randomly within a certain range.

For the intrinsic noise, it includes angle random walk and velocity random walk. It can be simply understood as Gaussian white noise, where white noise is a high-frequency error with a frequency much higher than the sampling frequency of the sensor, and it is a random fluctuation of the signal. The error caused by white noise to the gyroscope is called angular random walk (ARW), and the error units are rad/s/$\sqrt{\text{Hz}}$, deg/s/$\sqrt{\text{Hz}}$, deg/$\sqrt{\text{hr}}$. Assuming that the ARW of a device is 0.12 deg/$\sqrt{\text{hr}}$, it can be simply understood that within 1 hour, the ARW will cause an error of plus or minus $0.12°$. The error brought to the accelerometer is called velocity random walk (Vrw), and the unit of error is m/s$^2$/$\sqrt{\text{Hz}}$, m/s/$\sqrt{\text{h}}$, mGal/$\sqrt{\text{Hz}}$.

The scale factor error means the error of output measured signal/input physical quantity, and quadrature axis means the output of each axis is affected by the input of the other two axes, which will cause error. For the instability of zero bias, under fixed conditions (usually constant temperature), the change of the zero bias of the sensor within a specified period of time. It can be understood as the slow change of zero bias with time. If the zero bias is a certain value at the beginning, then after a period of time, the zero bias will change. The specific change is unpredictable. Therefore, it is necessary to give him a probability interval to describe how likely it is to fall within this interval. The longer the time, the larger the interval.

## VI. Budget

To comprehensively estimate the budget, it is necessary to include not only the costs of key components (such as LDV, MEMS accelerometer, and vibration exciter) but also the material and processing costs of installation tools, glue costs, wire costs, and peripheral equipment costs. The LDV model OFV5000 is priced at approximately CNY 181,050, with the actual price depending on the specific configuration chosen. For bulk purchases, such as when buying 62 units, the MEMS accelerometer model IIS2DH is priced at CNY 23.4 per unit. The vibration exciter JX-3B is priced at CNY 12,000. Installation tools, which consist of solid metal rods for machining flat surfaces, cost less than CNY 50. The cost of glue can be kept below CNY 40. Wires are relatively inexpensive, at approximately CNY 0.4 per unit, though a large quantity is needed. Peripheral equipment includes signal collectors, computers, and optical tables. These devices are expensive and typically reusable, so their costs are not included in the calculation. Depending on whether the LDV and JX-3B are used, the total budget is CNY 1,580 or CNY 194,630. The specific costs are detailed in Table IV.

TABLE IV
Budget for the measurement system

| Item | Unit price (CNY) | Quantity |
|---|---|---|
| MEMS accelerometer | 23.4 | 62 |
| LDV | 181,050 | 0 or 1 |
| Installation tool | 50 | 1 |
| Low viscosity glue | 15 | 1 |
| High viscosity glue | 25 | 1 |
| Flexible flat cable | 0.4 | 100 |
| JX-3B vibration exciter | 12,000 | 0 or 1 |
| Peripheral equipment | – | – |
| Total (without LDV) | CNY 1,580 | |
| Total (with LDV) | CNY 194,630 | |

## VII. Conclusion

This study investigated some advanced technologies for measuring vibrations that could be used in monitoring of nuclear fuel rods. We provide a full review and experimental evaluation of Fiber Bragg Grating (FBG) sensors, Laser Doppler Vibrometers (LDV), Micro-electromechanical Systems (MEMS) accelerometers, Eddy Current Sensors, and GRID method, illustrating in which high-precision vibration measurement applications each shines and its limitations. The results proved that the high-resolution vibration data generated by the LDV and MEMS accelerometers is useful, especially the LDV with the advantage of accurate non-contact measurement and MEMS sensors with the benefit of a great capacity for work in dynamic environments. More specifically, the laser Doppler vibrometer (LDV) was employed to determine the vibrational velocity magnitude of the glass wall and tracked the glass vibration at high spatial and temporal resolution for non-intrusive data acquisition without affecting the flow field. In the near field measurement, MEMS accelerometers were intentionally adhered to the inner surface of the rods in order to achieve full coverage of vibrations near the focal sphere in the origin.

The experimental setup and the data acquisition procedure guaranteed the reliability of the measurment synchronization, revealing the fundamental role of accuracy measurements, based on control of the experimental conditions and efficient systematic error compensation. The discovery furthers the importance of implementing advanced measurement methodologies in the comprehension of flow-induced vibrations in nuclear fuel rods, critically necessary for the structural integrity and safety of nuclear reactors.

In addition, future work should seek to combine these elements into a single, real-time monitoring and predictive maintenance capability, integrating the best features of the three technologies to enable fully spectral vibration analysis. Altogether, it possesses relevant results for vibration measurement techniques optimization, which may be beneficial in the near future for enhanced diagnostics and security purposes in nuclear energy applications.

## REFERENCES


[1] L. Wu, D. Lu, and Y. Liu, "Experimental investigation on flow-induced vibration of fuel rods in supercritical water loop," *Science & Technology of Nuclear Installations*, pp. 1–9, 2014.

[2] C. Dai, X. Wei, Y. Tai, and F. Zhao, "The optimum design of tight lattice reactor core with thin rod bundles," *Prog Nucl Energ*, vol. 59, pp. 49–58, 2012.

[3] A. Cioncolini, J. Silva-Leon, D. Cooper, M. K. Quinn, and H. Iacovides, "Axial-flow-induced vibration experiments on cantilevered rods for nuclear reactor applications," *Nuclear Engineering and Design*, vol. 338, pp. 102–118, Nov. 2018.

[4] B. Zhang, S. Gong, F. Gan, C. Zhang, and H. Gu, "Flow induced vibration measurement for a 4 × 4 rod bundle with spacer grids by the laser doppler vibrometer," *Annals of Nuclear Energy*, vol. 166, p. 108805, Feb. 2022.

[5] B. De Pauw, S. Vanlanduit, K. Van Tichelen, T. Geernaert, K. Chah, and F. Berghmans, "Benchmarking of deformation and vibration measurement techniques for nuclear fuel pins," *Measurement*, vol. 46, no. 9, p. 3647–3653, 2013.

[6] A. Bhattacharya and S. D. Yu, "An experimental investigation of effects of angular misalignment on flow-induced vibration of simulated candu fuel bundles," *Nuclear Engineering and Design*, vol. 250, pp. 294–307, Sep. 2012.

[7] G. Latimer, W. R. Marcum, T. K. Howard, W. Jones, A. M. Phillips, N. Woolstenhulme, S. Liu, A. Weiss, J. Campbell, M. Moussaoui, and C. Jensen, "On the flow induced vibration of an externally excited nuclear reactor experiment," *Nuclear Engineering and Design*, vol. 335, pp. 1–17, Aug. 2018.

[8] S. J. Rothberg, M. S. Allen, P. Castellini, D. Di Maio, J. J. J. Dirckx, D. J. Ewins, B. J. Halkon, P. Muyshondt, N. Paone, T. Ryan, H. Steger, E. P. Tomasini, S. Vanlanduit, and J. F. Vignola, "An international review of laser doppler vibrometry: Making light work of vibration measurement," *Optics and Lasers in Engineering*, vol. 99, pp. 11–22, Dec. 2017.

[9] C. Badulescu, M. Grédiac, J. D. Mathias, and D. Roux, "A procedure for accurate one-dimensional strain measurement using the grid method," *Experimental Mechanics*, vol. 49, no. 6, pp. 841–854, Dec. 2009.

[10] M. Varanis, A. Silva, A. Mereles, and R. Pederiva, "Mems accelerometers for mechanical vibrations analysis: A comprehensive review with applications," *Journal of the Brazilian Society of Mechanical Sciences and Engineering*, vol. 40, no. 11, p. 527, Oct. 2018.

[11] A. Othonos, K. Kalli, and G. E. Kohnke, "Fiber bragg gratings: fundamentals and applications in telecommunications and sensing," *Physics Today*, vol. 53, no. 5, pp. 61–62, 2000.

[12] J. García-Martín, J. Gómez-Gil, and E. Vázquez-Sánchez, "Non-destructive techniques based on eddy current testing," *Sensors*, vol. 11, no. 3, pp. 2525–2565, 2011.

[13] W. Niu, L. Fang, L. Xu, X. Li, R. Huo, D. Guo, and Z. Qi, "Summary of research status and application of mems accelerometers," *Journal of Computer and Communications*, vol. 06, no. 12, pp. 215–221, 2018.

[14] A. Mustafazade, M. Pandit, C. Zhao, G. Sobreviela, Z. Du, P. Steinmann, X. Zou, R. T. Howe, and A. A. Seshia, "A vibrating beam mems accelerometer for gravity and seismic measurements," *Scientific Reports*, vol. 10, no. 1, p. 10415, Jun. 2020.

[15] Y. Li, E. Dieussaert, and R. Baets, "Miniaturization of laser doppler vibrometers—a review," *Sensors*, vol. 22, no. 13, p. 4735, Jan. 2022.

[16] H. B. Mitchell, *Multi-sensor data fusion: an introduction*. Springer Science & Business Media, 2007.

[17] C. K. Chui, G. Chen *et al.*, *Kalman filtering*. Springer, 2017.

[18] HBKWorld. How does an optical strain gauge actually work? [Online]. Available: https://www.hbkworld.com/en/knowledge/resource-center/articles/strain-measurement-basics/optical-strain-sensor-fundamentals/article-how-does-an-optical-strain-gauge-actually-work#!ref_hbm.com

[19] C. Rembe and L. Mignanelli, "Introduction to laser-doppler vibrometry," in *Laser Doppler Vibrometry for Non-Contact Diagnostics*, K. Kroschel, Ed. Cham: Springer International Publishing, 2020, pp. 9–21.

[20] S. Sels, S. Vanlanduit, B. Bogaerts, and R. Penne, "Three-dimensional full-field vibration measurements using a handheld single-point laser doppler vibrometer," *Mechanical Systems and Signal Processing*, vol. 126, pp. 427–438, Jul. 2019.

[21] "Ldv principle / optolution." [Online]. Available: https://optolution.com/en/measuring-principles/ldv-principle/

[22] Dejan, "What is mems? accelerometer, gyroscope & magnetometer with arduino," Nov. 2015.

[23] L. e. a. Zhang, "Research on vibration fatigue test of alloy blade based on eddy current displacement sensor," *Tui jin ji shu 2*, p. 355, 2022.

[24] (2018) Induction of eddy currents by primary magnetic field. [Online]. Available: https://www.tec-science.com/material-science/material-testing/eddy-current-testing-ect/

[25] (2023) Principle, structure and characteristics of eddy current sensor. [Online]. Available: https://zhuanlan.zhihu.com/p/57150343

[26] Y. Surrel, "Moiré and grid methods: a signal-processing approach," in *Interferometry'94: photomechanics*, vol. 2342. SPIE, 1994, pp. 118–127.

[27] C. Lifante, B. Krull, Th. Frank, R. Franz, and U. Hampel, "3 × 3 rod bundle investigations, cfd single-phase numerical simulations," *Nuclear Engineering and Design*, vol. 279, pp. 60–72, Nov. 2014.

[28] A. Yang, S. Gong, and H. Gu, "An investigation of laser doppler vibrometer measurement technique on flow-induced vibration," *Journal of Test and Measurement Technology*, vol. 029, no. 002, pp. 93–99, 2015.

[29] Z. Y. ZOU Hong, "Error analysis in laser doppler measurement," *State Key Laboratory of Precision Measurement Technology and Instrument*, pp. 235–237, 2000.

[30] M. Leigh, "High power pulsed fiber laser sources and their use in terahertz generation," Jan. 2008.